ELSEVIER

Journal of Chromatography A 817 (1998) 253–262

JOURNAL OF CHROMATOGRAPHY A

Asymmetry of protein peaks in capillary zone electrophoresis: effect of starting zone length and presence of polymer

Sergey P. Radko[a], Andreas Chrambach[a,*], George H. Weiss[b]

[a]*Section on Macromolecular Analysis, Laboratory of Cellular and Molecular Biology, National Institute of Child Health and Development, National Institutes of Health, Building 10, Room 9D50, Bethesda, MD 20892-1580, USA*

[b]*Mathematical and Statistical Computing Laboratory, Center for Information Technology, National Institutes of Health, Building 12A, Room 2007, Bethesda, MD 20892-5620, USA*

Abstract

The asymmetry of R-phycoerythrin (M_r=240 000) peaks in capillary zone electrophoresis measured as $\ln[(t_m-t_1)/(t_2-t_m)]$, where t_m, t_1 and t_2 are migration times of the peak mode and at the intersection of the peak width at half-height with the ascending and descending limbs, respectively, was found to undergo a transition from negative to positive values with increasing starting zone length. The transition is compatible with a mathematical model of peak dispersion which assumes that an interaction of protein with the capillary walls governs the evolution of the peak during capillary zone electrophoresis. Models assuming a final peak shape defined solely by longitudinal diffusion, or by a heterogeneity with regard to mobility or by a conductivity difference between analyte zone and background electrolyte, have failed to give rise to a change in the sign of peak asymmetry when the starting zone length is varied. The presence of polyethylene glycol in the buffer within a concentration range up to 4% does not appreciably affect the peak asymmetry regardless of whether the concentration regime is dilute or semi-dilute. Above 4% of polyethylene glycol, the asymmetry becomes nearly independent of starting zone length, and progressively negative with increasing polymer concentration. The concentration range at which the transition from negative to positive asymmetry disappears coincides with that at which the average mesh size of the polymer network falls below the size of the protein. © 1998 Published by Elsevier Science B.V.

Keywords: Band profiles; Buffer composition; Proteins

1. Introduction

An understanding of the mechanisms leading to peak asymmetry in capillary zone electrophoresis (CZE) and the consequent peak spreading is important for the practice of separations since separation efficiency defined in terms of plate height or theoretical plate number is a function of the increasing peak width with migration time (distance). Peak tailing and asymmetry has been qualitatively observed in numerous previous reports (e.g., [1–5]). It has been assumed that these observed features of the peaks were due to either electromigration dispersion ([6] and references therein) or interaction of the analyte with the capillary wall ([7] and references therein). These two potential sources of peak asymmetry have been theoretically investigated, that in relation to the conductance difference between analyte and buffer by one group of authors ([6] and references given therein) and that in relation to interaction of the analyte with the capillary wall by other authors [7,4]. Surprisingly, no previous systematic and/or quantitative experimental studies of peak shape in CZE have been carried out.

*Corresponding author.

0021-9673/98/$19.00
PII: S0021-9673(98)00470-1

The present work attempts to systematically investigate the relation between peak asymmetry and a widely varied and disregarded parameter relevant to it, viz. starting zone length, in the CZE of proteins in presence and absence of a polymeric sieving medium. That investigation used R-phycoerythrin of M_r=240 000 as a representative protein and a solution of polyethylene glycol (PEG) as a polymeric medium.

2. Experimental

2.1. Materials

2.1.1. Buffer

(2-[*N*-cyclohexylamino]-ethanesulfonic acid) (CHES, Sigma, St. Louis MO, USA, Cat. No. C-2885) was used to prepare Tris–CHES buffer (50 m*M* Tris, 25 m*M* CHES, pH 9.0).

2.1.2. Polymer

Polyethylene glycol (PEG) with M_r 20 000, 40 000, 100 000, 200 000, 300 000, 400 000 and 4 000 000 was obtained from Sigma. The polymer was dissolved with gentle agitation for 0.5 to 3 days, depending on its M_r, in deionized water. The PEG solutions in buffer were obtained by mixing the resulting aqueous solution with a 10-fold concentrate of the buffer.

2.1.3. Protein

The naturally fluorescing protein, R-phycoerythrin (M_r 240 000) was obtained from Polysciences (Warrington, PA, USA, Cat. No. 18188). The commercial suspension of R-phycoerythrin in ammonium sulfate was centrifuged at about 2000 *g*. The pellet was dissolved to 10 mg/ml in Tris–CHES buffer. A 1/1000 dilution in the same buffer served as the sample, except in the experiments reported in Section 3.3.

2.1.4. Electroendosmosis marker

Mesityl oxide (Aldrich, Milwaukee, WI, USA, Cat. No. 141–79–7) was used.

2.2. Capillary electrophoresis

CZE was carried out in the HPCE-2100 apparatus (Beckman Instruments, Fullerton, CA, USA), using a fluorescence detector as described [8]. The procedure of pressure injection and CZE was that specified previously [9]. The Tris–CHES buffer (Section 2.1) was used. The polymer dissolved in the buffer in the pertinent experiments (see Results) was PEG with M_r listed in Section 2.1. Capillary lengths of 27, 47 and 57 cm and a diameter of 100 μm were used. Capillaries were internally coated with 3 polyacrylamide [10]. Electroendosmosis in the buffer was measured as the retention time of mesityl oxide (0.05%) loaded from the anodic reservoir. Capillaries exhibiting electroendosmosis in excess of 1×10^{-5} cm^2 s^{-1} V^{-1} (4% of the mobility of phycoerythrin) were discarded.

2.3. Data processing

The relative length of the injected sample zone, L_o/L, was calculated as described, where L_o designates the starting zone length, L the capillary length from origin to detector [8]. Asymmetry was measured as $\alpha=\ln(\Delta t_1/\Delta t_2)$, where $\Delta t_1=(t_m-t_1)$ and $\Delta t_2=(t_2-t_m)$ (Fig. 1).

3. Results

3.1. Transition from negative to positive asymmetry of the R-phycoerythrin peak with an increase in starting zone length

As the length of the starting zone, L_o, is increased, the asymmetry of the R-phycoerythrin peak changes from a progressive decrease of negative asymmetry to a progressively increasing positive asymmetry (Fig. 2). The transition is independent (within experimental range and scatter) of capillary length (Fig. 2A).

3.2. No effect of PEG below a concentration of 4% on the dependence of the asymmetry of the R-phycoerythrin peak on starting zone length in CZE

Below a concentration of 4%, the addition of 1% PEG (20 000–4 000 000) (Fig. 2) or 4% PEG (20 000–400 000) (Fig. 2) to the buffer has no effect (within experimental range and scatter) on the depen-

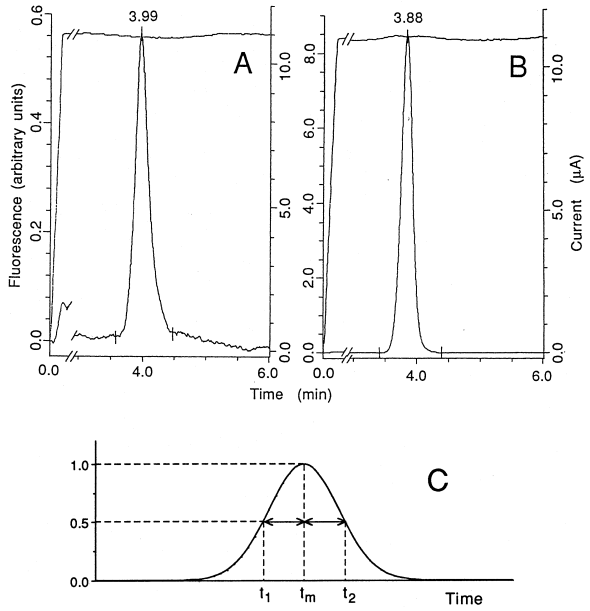

Fig. 1. Representative CZE patterns and schematic diagram defining positive and negative asymmetry. (A) CZE (0.025 *M* CHES, 0.05 *M* Tris, pH 9.0, 25°C, 370 V/cm, effective capillary length 200 mm, total capillary length 270 mm) pattern of R-phycoerythrin (10 μg/ml); calculated starting zone length 0.42 mm. (B) As (A) except that the starting zone length is 6.2 mm. (C) Schematic diagram of a CZE peak. Asymmetry $\alpha = \ln(\Delta t_1 / \Delta t_2)$, where $\Delta t_1 = t_m - t_1$ and $\Delta t_2 = t_2 - t_m$. The sign of α defines positive and negative asymmetry.

dence of the asymmetry of the protein peak on starting zone length. By contrast, when the PEG concentration exceeds 4%, the asymmetry of the protein peak becomes independent of the length of the starting zone (Fig. 2).

3.3. Dependence of peak asymmetry and peak spreading on sample concentration

Peak asymmetry is independent of R-phycoerythrin concentration up to 0.1 mg/ml (Fig. 3) within the limits of experimental scatter.

3.4. Prediction on the basis of various theoretical models of the relation between starting zone length and peak asymmetry:

The transition from negative to positive asymmetry with increasing starting zone length demonstrated experimentally (Section 3.1) is consistent with a model which assumes a reversible adsorption of the analyte to a component of the capillary walls. By contrast, models which solely assume diffusion, a mobility heterogeneity or a concentration dependent mobility (electrophoretic dispersion) do not predict a change in sign of the asymmetry as a function of starting zone length (Appendix A).

4. Discussion

4.1. Relation between peak asymmetry in spatial and temporal units

CZE is known to possess a peculiar feature: even a peak which in spatial units is perfectly symmetrical may appear asymmetric on the temporal scale. This is due to the difference in velocity of species along the trailing and leading limbs of a peak passing across the detector. Assuming an infinitely narrow starting zone (i.e. a migration of all species from the identical initial position), the relation between asymmetry in spatial and temporal units is

$$\Delta X_1 / \Delta X_2 = \Delta t_1 / \Delta t_2 \times t_2 / t_1 \quad (1)$$

where ΔX_1 and ΔX_2 denote the difference between the migration distance at the peak mode and that at the half-height of descending and ascending limbs, respectively, when the spatial position of the peak mode coincides with a detector position. For a symmetric peak,

$$\Delta X_1 = \Delta X_2 \quad (2)$$

and therefore Eq. (1) may be rearranged as

$$\Delta t_1 / \Delta t_2 = t_1 / t_2 \quad (3)$$

Since $t_1 / t_2 < 1$ (Fig. 1), a symmetric peak always shows a negative asymmetry on the temporal scale (measured as described in Section 2.3) and moreover, the degree of asymmetry increases with peak width. This results in the solid line depicted in Fig. 4. All points along that line correspond to symmetric peaks of different widths. By contrast, all points in Fig. 4 which do not lie on the line, reveal a true asymmetry of the peaks. Such is the case for the experimental values obtained in this study which are shown as open circles in Fig. 4. The values corre-

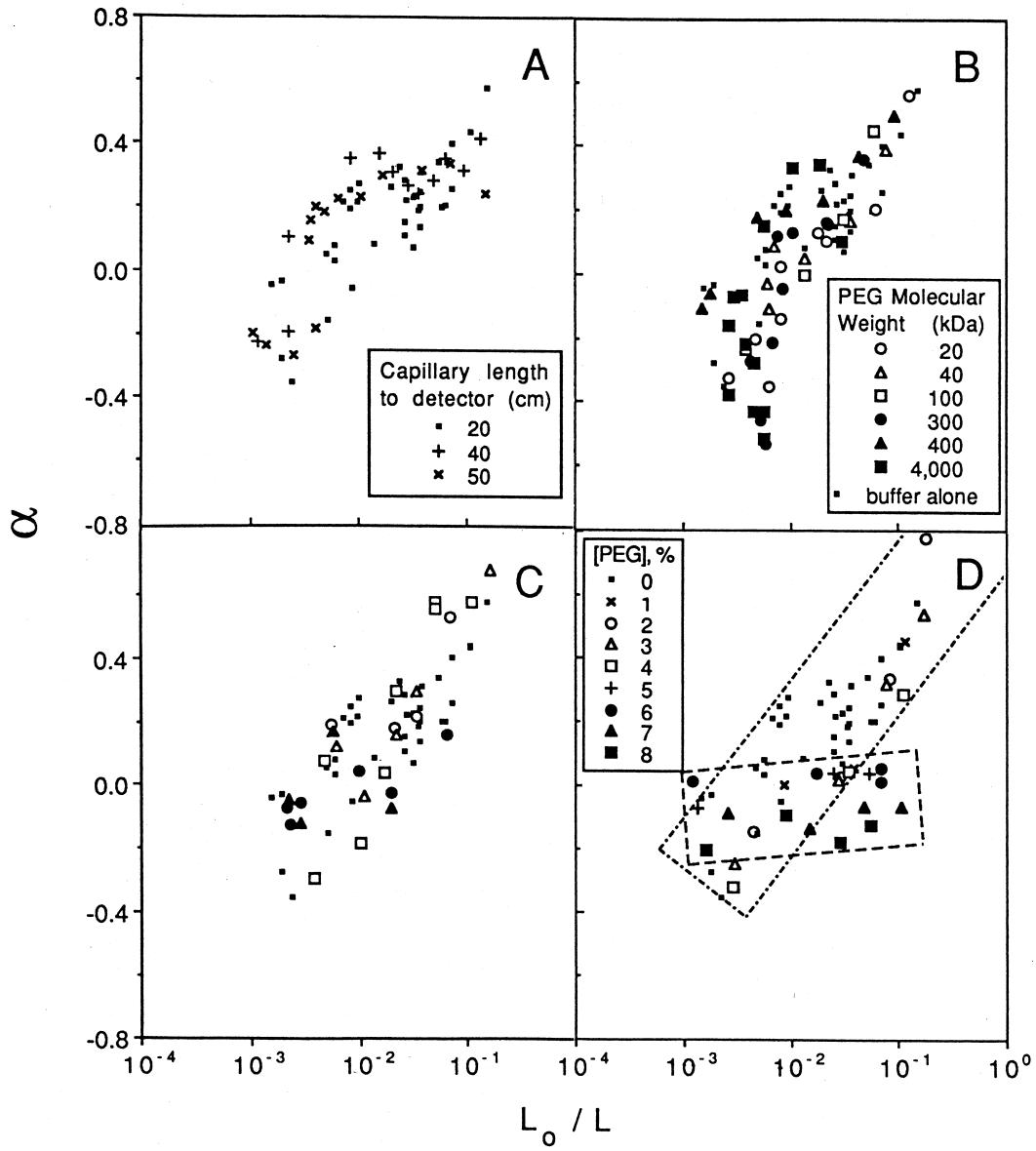

Fig. 2. Peak asymmetry in CZE as a function of starting zone length. L_o/L = starting zone length relative to effective capillary length. (A) CZE in buffer; variation of effective capillary length. (B) CZE in buffered 1% polyethylene glycol (PEG) solutions; effective capillary length = 200 mm; variation of the size of PEG. (C) As (B) except 4% PEG. (D) As (B) except at various concentrations of PEG with M_r = 200 000. Other conditions as in Fig. 1.

spond to starting zones within 0.1–1% of the effective capillary length, i.e. they are sufficiently narrow to be compatible with the assumption of infinitely narrow starting zone lengths in Eq. (1).

4.2. Relation between peak asymmetry and starting zone length

In general, the conversion of a temporal scale into

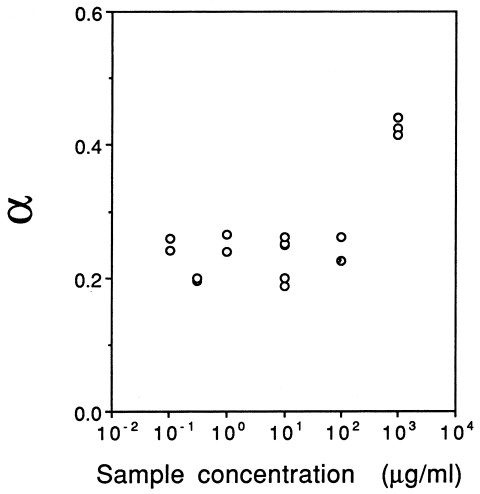

Fig. 3. Peak asymmetry as a function of R-phycoerythrin concentration. Conditions as in Fig. 1.

a spatial one cannot be carried out due to the uncertainty in the migration distance when the starting point of the migration cannot be defined. Thus, the parameter α which has been used to study the peak asymmetry as a function of starting zone length necessarily employs temporal units.

As shown in Fig. 2, the peak asymmetry of phycoerythrin undergoes a transition from positive values to negative ones when the relative length of starting zone decreases. To account for the observed transition, several models have been analyzed as described in Appendix A. Each model considers the peak shape evolution as a result of the following dispersive processes: (i) longitudinal diffusion by itself; (ii) longitudinal diffusion in conjunction with conductance differences between the analyte zone and background electrolyte; (iii) longitudinal diffusion in conjunction with heterogeneity of mobility; (iv) interaction between analyte and capillary walls. The conductance differences are known to result in either an elevation or a reduction of electric field strength in the analyte zone compared to that in the surrounding buffer [11]. It gives rise to negative or positive (as defined in Fig. 1) asymmetry, respectively. While the direction of change in field strength (elevation or reduction) is a function of the relation between effective mobilities of the analyte and electrolyte co-ions, its extent is assumed to be directly proportional to analyte concentration [6,11,13]. Since peak asymmetry demonstrates a positive increase with protein concentration (Fig. 3), one may assume that the field strength is rather reduced in the analyte zone. Thus, the impact of the conductance differences on peak asymmetry was analyzed by using a mobility, μ, dependent of analyte concentration, c, in the form $\mu=\mu_0(1-\varepsilon c)$ where μ_0 and ε are constants; it should be noted that $\varepsilon>0$ (see Appendix A).

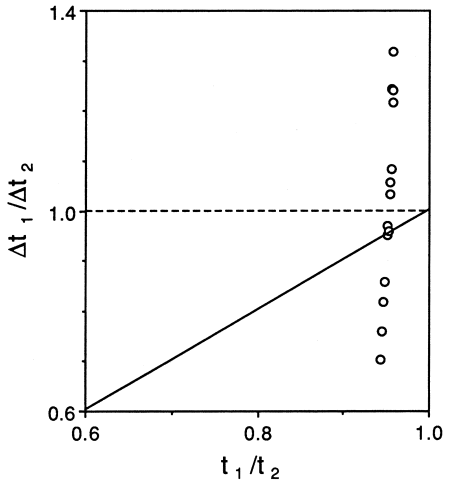

Fig. 4. Deviation from the line described by Eq. (3) as a criterion for non-artifactual peak asymmetry.

It was found that the only model able to generate a change in the sign of α is that postulating an interaction of the analyte with the capillary walls (Fig. 5). The model is formulated in terms of a non-Markovian generalization of one originally analyzed by Giddings and Eyring [12]. This model postulates that a single analyte molecule can find itself in one of two phases, mobile or immobile. In the mobile phase the molecule is assumed to diffuse by Brownian motion; in the immobile phase it remains stationary except for thermal fluctuations which eventually return the molecule into the mobile phase. Under conditions of an analyte within a capillary internally coated with polyacrylamide and filled with a buffer of relatively high alkaline pH, as in the present study, the immobile phase is likely to result from a reversible adsorption of the protein due

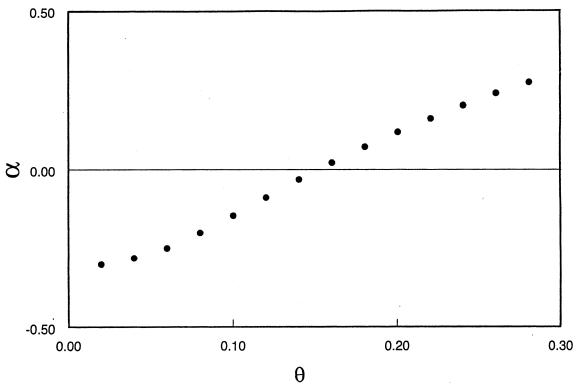

Fig. 5. Computer simulated peak asymmetry, calculated on the basis of Eq. (A12), as a function of relative starting zone length. The relative starting zone length L_o/L is described by dimensionless parameter Θ (Eq. (A3)). $\beta=0.05$, $z=0.1$ (see Eq. (A12)).

to hydrophobic and/or hydrogen bond interactions with the silica walls of the capillary or an entanglement with the polymeric layer in the vicinity of the capillary walls. Irrespective of the physical source of the immobile phase, the transition between mobile and immobile phases may be described in terms of a probability density for a single interaction time, i.e., the probability for a single molecule to spend a particular fraction of the time in the stationary state. Thus, both peak shape and dispersion are attributed to the random times spent by analyte molecules in the stationary state rather then to longitudinal diffusion. The model applies to any analytes capable of a reversible interaction with the capillary wall. That interaction at equilibrium provides retention, but not band spreading or asymmetry. Therefore, the application of the model to account for band spreading and asymmetry assumes an interaction which results in non-equilibrium conditions. A detailed discussion of the model can be found in [14] and its application to the particular case of a non-zero starting zone length is given in Appendix A.

4.3. Spontaneous (''ubiquitous'') injection and peak asymmetry

Spontaneous or ''ubiquitous'' injection was first reported by Grushka and McCormick [15]. They found that, by simply dipping a capillary end into a sample solution, small amounts of the sample can be injected. This extraneous injection is always present superimposed on an electrokinetic or hydrostatic injection and it alone appears to provide the smallest possible starting zones. However, the observed peaks were quite broad [15]. Later Cohen and Glushka have shown [16] that the physical shape of the capillary inlet (straight-edge or slanted edge) can severely affect the performance efficiency and peak shape: slanted edge capillaries yielded less efficient electropherograms and gave negatively (if measured as in Section 2.3) asymmetric peaks. Moments analysis carried out by the authors [16] has shown that the expected increase in the size of the injected plug due to the slanted shape of the capillary inlet can explain neither the large decrease in efficiency nor the peak asymmetry. As noted in the last review by Gas et al. on peak broadening in CZE, the observed phenomenon is still puzzling [17].

The mechanisms of spontaneous injection were experimentally and theoretically analysed by Fishman et al. [18]. These authors have demonstrated that such injection is caused primarily by an interfacial pressure difference across a droplet formed at the inlet of the capillary upon removal from a sample reservoir. The injection length was found to be a function of a number of parameters including delay between sample introduction and reinsertion into the inlet (e.g., electrolyte containing) reservoir, the shape of capillary end, and even the speed at which the capillary leaves the sample solution (the latter affects the size of droplet) [18].

The present study suggests that the peak broadening and asymmetry observed upon spontaneous injections can be a result of the starting zone approaching zero length. The effect of starting zone length on peak width in CZE has been recently studied both experimentally and theoretically [8]. Suprisingly, the solution obtained for the standard diffusion equation but with non-local initial analyte concentration (non-zero starting zone length) demonstrates that peak width has to have a minimum at a finite starting zone length, i.e., the further approach of starting zone towards zero length can result in monotonic increase of peak width that was indeed observed experimentally [8]. The present work shows that if there exists an interaction between analyte molecules and capillary walls which may be described in terms of the ''mobile–immobile phase''

model (see above), then negatively asymmetric peaks are likely to appear at small starting zone lengths. That can explain the peak asymmetry observed in [16], since slanted edge capillaries are likely to produce smaller injection plugs than straight-edge ones under the same conditions [18].

4.4. Peak asymmetry in the presence of polymer in the buffer

In CZE polymer solutions are mostly used in two concentration regimes: dilute and semi-dilute (e.g., [19]). In a dilute solution polymer coils are separated in space and interact incidentally. When the polymer concentration is increased, at some point (the so-called ''entanglement threshold'', c^*) the polymer coils start to overlap and penetrate into each other. The entanglement threshold decreases with polymer size (molecular mass, M_r). Above c^* the coils form a continuous network due to spatial interaction between polymer chains (semi-dilute regime). Once formed, the network is characterized by an average size of mesh which decreases with polymer concentration and is independent of polymer molecular weight (e.g., [19]).

A polymer network in solution can be generated either by increasing the concentration of a polymer of defined M_r, or by increasing the M_r of the polymer at a defined concentration. For PEG the transition points can be calculated accordingly [8] as $M_r =$ 250 000 and 40 000 at $c = 1$ and 4%, respectively. As seen from Fig. 2, both the presence of polymers and the network formation do not affect the peak asymmetry appreciably within this concentration range. However, above 4% of PEG (Fig. 2) the behavior changes dramatically: The dependence on starting zone length becomes much weaker and the values of asymmetry are shifted downwards with increasing polymer concentration. As shown in [8], above a polymer concentration of 4–5% the size of R-phycoerythrin starts to exceed the average size of mesh of the polymer network, and correspondingly a transition occurs from an occupancy mechanism (the protein particle interacts with the polymer network through the occupancy of spaces in the network) to a network displacement mechanism (one of local displacement of the network by the particle) [20]. One may assume that the kinetics of transition between ''mobile'' and ''immobile'' phase (see Section 4.2 and Appendix A) greatly differ under the latter mechanism resulting in the observed change in peak asymmetry dependencies on starting zone length at PEG concentrations above 4% (Fig. 2).

5. Conclusion

The shape of R-phycoerythrin peaks in CZE under conditions used demonstrates a transition between two opposite types of asymmetry as a function of starting zone length. It is assumed in this regard that R-phycoerythrin is a representative protein. The transition is compatible with a mathematical model assuming that an interaction of protein molecules with a component of the capillary wall defines a final peak shape but incompatible with models assuming that the asymmetry is defined by longitudinal diffusion, a mobility heterogeneity or conductivity differences between analyte zone and background electrolyte. The presence of polymer (polyethylene glycol) in the buffer does not appreciably affect the peak asymmetry unless the size of the protein exceeds the average mesh size of the polymer network.

Appendix A

Possible mechanisms for peak asymmetry

We have examined several models of diffusion in CZE to determine whether any of them leads to a transition in the sign of asymmetry, as defined in terms of $\alpha = \log(\Delta t_1/\Delta t_2)$, where the definitions of Δt_1 and Δt_2 are defined in Fig. 1. The first model considered was that of the standard diffusion in which the evolution of the peak is governed by the equation

$$\frac{\partial c}{\partial t} = D\frac{\partial^2 c}{\partial x^2} - \mu E\frac{\partial c}{\partial x} \tag{A1}$$

where D is the diffusion constant, μ the mobility, and E is the electric field. Eq. (A1) is to be solved subject to the initial condition

$$c(x,0)=\begin{cases}1, & 0\le x_0\le L_0<L\\ 0, & x>L_0\end{cases} \quad \text{(A2)}$$

where $x=L$ is the point at which the concentration is measured as a function of time.

To analyze the solution to Eq. (A1) it is convenient to introduce the dimensionless variables

$$\tau=\mu Et/L,\ y=x/L,\ \mathscr{D}=D/(\mu EL),\ \theta=L_0/L \quad \text{(A3)}$$

which converts Eq. (A1) into

$$\frac{\partial c}{\partial \tau}=\mathscr{D}\frac{\partial^2 c}{\partial y^2}-\frac{\partial c}{\partial y} \quad \text{(A4)}$$

with the initial condition, $c(y,0)=1$ for $0\le y\le\theta$ and $=0$ otherwise. Thus, we have reduced the number of parameters to $\mathscr{D}$ and θ. The solution to Eq. (A4) with the stated initial condition is readily shown to be

$$c(y,\tau)=\frac{1}{2}\left[\operatorname{erf}\left(\frac{\tau-1+\theta}{\sqrt{4\mathscr{D}\tau}}\right)-\operatorname{erf}\left(\frac{\tau-1}{\sqrt{4\mathscr{D}\tau}}\right)\right] \quad \text{(A5)}$$

in which

$$\operatorname{erf}(z)=\frac{2}{\sqrt{\pi}}\int_0^z e^{-u^2/2}\,du \quad \text{(A6)}$$

In the set of units defined in Eq. (A3) the measured quantity is $c(1,\tau)$, whose maximum c_{max} occurs at $\tau=\tau_{max}$, which is easily determined numerically from the expression in Eq. (A5). Two values of τ, designated as τ_- and τ_+ were then determined as the two solutions of the equation

$$c(1,\tau)=c_{max}/2 \quad \text{(A7)}$$

so that $\Delta\tau_1=\tau_{max}-\tau_-$ and $\Delta\tau_2=\tau_+-\tau_{max}$. A numerical investigation over a physically realistic range of $\mathscr{D}$ indicates that the separation ratio α plotted as a function of θ always remains negative, in contrast to the experimentally observed results which indicates that the sign does indeed change as θ changes.

A model which has been shown to lead to qualitative agreement with peak symmetry in gel electrophoresis is a non-Markovian generalization of a model originally proposed by Giddings and Eyring [12]. The non-Markovian model was originally proposed in Ref. [21] and is briefly summarized and compared with experimental data in Ref. [22]. The basic idea behind the model is that at any time t a molecule can be regarded as being either mobile or stationary, either because it is entangled with the gel in gel electrophoresis, or due to interaction with the wall in CZE. The assumption that diffusion can be neglected for mobile molecules, which is supported by the data in [22], then replaces the diffusion equation (Eq. (A1)) by a nonlocal equation of the form

$$\frac{\partial c(x,t)}{\partial t}=-\mu E\int_0^t Q(t-\tau)\frac{\partial c(x,\tau)}{\partial x}\,d\tau \quad \text{(A8)}$$

where $Q(t)$ is a function which summarizes information about kinetics of transitions between the mobile and entangled states.

When, initially, $c(x,0)=\delta(x)$, one can solve Eq. (A8) for the Laplace transform of the concentration, i.e.,

$$\hat{c}(x,s)=\int_0^\infty c(x,t)e^{-st}dt \quad \text{(A9)}$$

The solution can be expressed in terms of the Laplace transform of $Q(t)$, $\hat{Q}(s)$ as

$$\hat{c}(x,s)=\frac{1}{\mu E\hat{Q}(s)}\exp\left(-\frac{sx}{\mu E\hat{Q}(s)}\right) \quad \text{(A10)}$$

From this relation one can calculate the Laplace transform of the concentration that results from the initial condition in Eq. (A2) which now takes the form

$$\hat{c}(x,s)=\frac{1}{s}\exp\left(-\frac{sL}{\mu E\hat{Q}(s)}\right)\left[\exp\left(\frac{sL_0}{\mu E\hat{Q}(s)}\right)-1\right] \quad \text{(A11)}$$

The result in this last equation is exact. To make further progress one needs to make some assumptions about the form of $\hat{Q}(s)$. Details of the required assumption as well as a justification in terms of a kinetic model are to be found in Refs. [21,22] to which the reader is referred. In the type of model used to fit data described in Ref. [22], we are able to reduce Eq. (A11) to an equivalent Laplace transform which is

$$\hat{c}(z, s) = \frac{A}{s} \exp\left(-\frac{z}{1+s^{\beta}}\right)\left[\exp\left(\frac{z\theta}{1+s^{\beta}}\right) - 1\right] \quad \text{(A12)}$$

where A is a constant, z is a dimensionless variable proportional to the distance from $x=0$, s is the Laplace transform parameter, and β is a model parameter which is positive and less than 1. Fig. 5 shows a plot of α as a function of θ for $\beta=0.025$ and $z=0.1$. While the shape of the curve is not convex over the whole range as is true in the experimental data, it is the only evidence available to us at present that there are models capable of generating a crossover in sign for the parameter α. The crucial point is that we have postulated a specific form for $\hat{Q}(s)$ which encapsulates the kinetics of entanglement times. There is some freedom in this choice allowing us to presume that another choice of this transform might lead to a curve that more closely resembles experimental results. Fig. 6 shows the actual shapes of the two peak profiles for $\theta=0.05$ and 0.30 obtained from Eq. (A12) by numerical inversion of the Laplace transform. One observes that when $\theta=0.05$ the rectangular initial profile is no longer in evidence, while when $\theta=0.30$ a distinct signature of the initial profile remains.

We examined two other possible causes of asymmetry, the first being a distribution, rather than a single value, of the mobility, and the second being a concentration-dependent mobility, i.e., $\mu=\mu_0(1-\varepsilon c)$, where μ_0 and ε are constants. Both of these cases can be analyzed exactly – in the first it is only necessary to solve Eq. (A1) and average with respect to the probability density of the mobility, and second requires generating a solution for the nonlinear Burger's equation [23,24]. When dealing with heterogeneous mobility we only examined density of the form

$$g(\mu) = \begin{cases} \dfrac{1}{2\Delta\mu}, & \mu_0 - \Delta\mu \le \mu \le \mu_0 + \Delta\mu \\ 0 & \text{otherwise} \end{cases} \quad \text{(A13)}$$

We were not able to produce a change in the sign of α with either of these two models. Of course, it is impossible to rule out the possibility of finding such a change with some other form of mobility density or nonlinearity, but the fact that the generalized Giddings–Eyring model reproduces many qualitative features of gel electrophoretic data makes it a viable contender for application to the present set of CZE data.

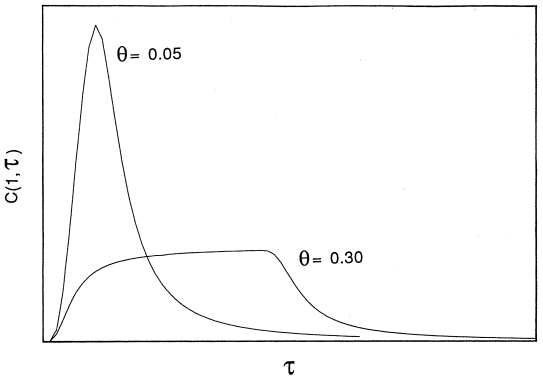

Fig. 6. Computer simulated peak profiles $c(1,\tau)$ calculated on the basis of Eq. (A12) for a relative starting zone length $\Theta=0.05$ and 0.30 with $\beta=0.025$ and $z=0.1$.

References

[1] H.H. Lauer, D. McManigill, Anal. Chem. 58 (1986) 166.
[2] K.A. Cobb, V. Dolnik, M. Novotny, Anal. Chem. 62 (1990) 2478.
[3] J.-L. Viovy, F. Miomandre, M.-C. Miquel, F. Caron, F. Sor, Electrophoresis 13 (1992) 1.
[4] B. Gas, M. Stedry, A. Rizzi, E. Kenndler, Electrophoresis 16 (1995) 958.
[5] G.M. Slater, Electrophoresis 14 (1993) 1.
[6] P. Gebauer, P. Bocek, Anal. Chem. 69 (1997) 1557.
[7] S.V. Ermakov, M.Yu. Zhukov, L. Capelli, P.G. Righetti, J. Chromatogr., A 699 (1995) 297.
[8] S.P. Radko, G.H. Weiss, A. Chrambach, J. Chromatogr. A 781 (1997) 277.
[9] S.P. Radko, M.M. Garner, G. Caiafa, A. Chrambach, Anal. Biochem. 223 (1994) 82.
[10] S. Hjerten, J. Chromatogr. 347 (1985) 191.
[11] F.E.P. Mikkers, F.M. Everaerts, Th.P.E.M. Verheggen, J. Chromatogr. 169 (1979) 1.
[12] J.C. Giddings, H. Eyring, J. Phys. Chem. 59 (1955) 416.
[13] X. Xu, W.Th. Kok, H. Poppe, J. Chromatogr. A 742 (1996) 211.
[14] G.H. Weiss, H. Sokoloff, S.F. Zakharov, A. Chrambach, Electrophoresis 17 (1996) 1325.

[15] E. Grushka, R.M. McCormick, J. Chromatogr. 471 (1989) 421.
[16] N. Cohen, E. Grushka, J. Chromatogr. A 684 (1994) 323.
[17] B. Gas, M. Stedry, E. Kenndler, Electrophoresis 18 (1997) 2123.
[18] H.A. Fishman, N.M. Amudi, T.T. Lee, R.H. Scheller, R.N. Zare, Anal. Chem. 66 (1994) 2318.
[19] J.-L. Viovy, T. Duke, Electrophoresis 14 (1993) 322.
[20] S.P. Radko, A. Chrambach, Electrophoresis 17 (1996) 1094.
[21] G.H. Weiss, Sep. Sci. Technol. 17 (1982) 1609.
[22] E. Yarmola, P.P. Calabrese, A. Chrambach, G.H. Weiss, J. Phys. Chem. B101 (1997) 2381.
[23] G.B. Whitham, Linear and Nonlinear Waves, Wiley, New York, 1974.
[24] I.H. Billick, G.H. Weiss, Nature 201 (1964) 792.